PHOENICS Newsletter

CHAM

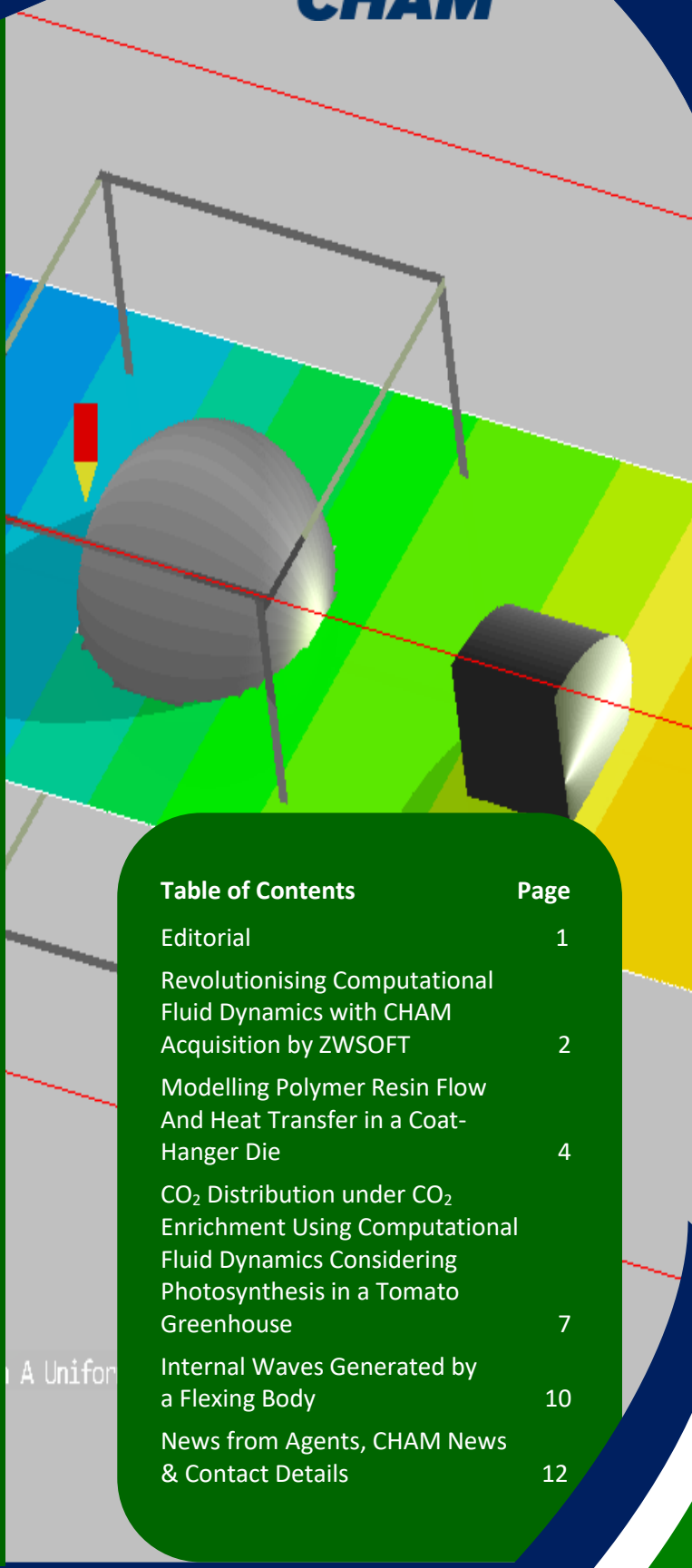

As of October 2, CHAM was purchased by ZWSOFT a CAx Company based in China. Agreement was reached between the ZWSOFT CEO (Trumann Du) and myself at end April this year. Subsequently, there were stages to be worked through to ensure the continued successful future of CHAM Staff, PHOENICS, the Agent network, etc.

The team at CHAM is skilled in what it does. John Ludwig and Steve Mortimore took on code development after Brian's death. User Support is in the capable hands of Mike Malin. John and Mike have been part of the CHAM story for over 40 years with Jill Rayss, Emma Jureidini and Michelle Lyle not far behind. The company is what it is because of all our staff. It became clear, however, that colleagues would leave (indeed Peter Spalding left in April) and that PHOENICS would benefit from new minds trained in CFD, a link to CAD software and more extensive marketing. From my CHAM viewpoint, therefore, the decision to sell was made to optimize the future of CHAM's greatest assets: its staff (above), PHOENICS, and Brian Spalding's CFD legacy.

At the behest of ZWSOFT, my 50 years with CHAM will end in December. It has been an incredible experience – not to be missed. My thanks and gratitude go to all with whom I have worked. I will treasure my memories of the people, and the times, as CHAM moves into a new era.

Thank you - and here is to the future - Colleen Spalding

Table of Contents **Page**

Editorial 1

Revolutionising Computational Fluid Dynamics with CHAM Acquisition by ZWSOFT 2

Modelling Polymer Resin Flow And Heat Transfer in a Coat-Hanger Die 4

CO_2 Distribution under CO_2 Enrichment Using Computational Fluid Dynamics Considering Photosynthesis in a Tomato Greenhouse 7

Internal Waves Generated by a Flexing Body 10

News from Agents, CHAM News & Contact Details 12

Concentration, Heat and Momentum Limited (CHAM)
Bakery House, 40 High Street, Wimbledon Village, London, SW19 5AU, England
Tel: +44 (0)20 8947 7651 Email: phoenics@cham.co.uk Web: www.cham.co.uk

Autumn 2023

Revolutionizing Computational Fluid Dynamics with CHAM Acquisition by ZWSOFT

Jalil Ouazzani, ArcoFluid Consulting (Orlando, Florida) & ArcoFluid (Bordeaux, France)

ArcoFluid and ArcoFluid Consulting are thrilled to learn of a groundbreaking development in the realm of Computational Fluid Dynamics (CFD) that is set to redefine industry standards. Building on CHAM's rich legacy as a trailblazer in CFD since 196974, we are excited about the strategic alliance by which CHAM has been acquired by ZWSOFT, a leading provider of comprehensive Computer-Aided Design (CAD) solutions, marking a pivotal moment in the future of CFD innovation

At the core of this collaboration lies the fusion of CHAM's unparalleled PHOENICS CFD engine and ZWSOFT's advanced CAD capabilities. This powerful combination merges cutting-edge technology and expertise, propelling PHOENICS to the forefront of the CFD market. PHOENICS, a pivotal tool for numerous industries since its inception in 1981, has facilitated groundbreaking innovations and solutions.

ArcoFluid, and ArcoFluid Consulting, have cooperated in expanding PHOENICS' horizons and providing unparalleled support to our loyal user base. We look forward to working with CHAM and ZWSOFT to share in a vision which extends beyond a simple transition; it heralds the dawn of an era marked by innovation and excellence.

In the domain of multiphase flow, ArcoFluid and ArcoFluid Consulting have worked with CHAM to introduce comprehensive developments in the free surface world of CFD, including:

Multiphase Electro-Coalescence Models: Advancing the understanding of multiphase interactions

Multiphase electro-coalescence in the context of Computational Fluid Dynamics (CFD) refers to the simulation and analysis of the behaviour of multiple immiscible fluid phases, such as oil and water, under the influence of an electric field to promote coalescence, where droplets of one phase merge with droplets of another phase. This phenomenon has significant applications in various fields, including petroleum engineering, chemical processes, and environmental engineering.

Here's an overview of the key aspects of CFD modelling for multiphase electro-coalescence:

- **Phases:** phases, typically oil and water, are simulated as distinct entities within the computational domain.
- **Interfacial Dynamics:** CFD models capture the interactions at the interface of different phases, considering surface tension, contact angles, and electrostatic forces.
- **Electric Potential:** The electric field is represented by the distribution of electric potential within the domain.
- **Electrostatic Forces:** CFD models incorporate electrostatic forces acting on the droplets, influencing their movement and coalescence behaviour.
- **Coalescence:** CFD models study conditions under which droplets merge due to the influence of the electric field, leading to the formation of larger droplets.
- **Breakup:** Conversely, the models also explore scenarios where larger droplets break into smaller ones due to various factors, including turbulence or opposing forces.
- **Oil-Water Separation:** In petroleum engineering, multiphase electro-coalescence is used to enhance oilwater mixture separation, improving the efficiency of oil recovery processes.
- **Emulsion Breakdown:** In Chemical engineering there are applications in breaking down emulsions for various industrial processes.
- **Environmental Remediation:** Multiphase electro-coalescence can be applied to treat wastewater contaminated with oils and suspended solids.

Multiphase Evaporation and Condensation Models: Enabling precise modelling of phase changes

CFD simulations of multiphase evaporation and condensation are essential to understand the complex phenomena involved in phase change processes in fields such as heat exchangers, refrigeration systems, and environmental engineering.

- **Phases:** CFD models consider multiple phases, such as liquid and vapor, and possibly other phases like solid particles if applicable (for example, in spray drying processes).
- **Phase Change:** The phase change between liquid and vapor is simulated using appropriate mathematical models, capturing the energy exchange during evaporation and condensation.
- **Heat Transfer:** CFD models heat-transfer mechanisms, including conduction, convection, and radiation, which influence evaporation and condensation rates.
- **Mass Transfer:** Mass transfer between liquid and vapor phases is modelled based on principles of diffusion and phase- change kinetics.
- **Vapor Species:** If the condensing or evaporating substance involves multiple chemical species, CFD models track the transport and phase change of each species separately. This is common in processes involving mixtures or pollutants.
- **Interfacial Area:** CFD simulations calculate the interfacial area between liquid and vapor phases, which is crucial for accurate modelling of phase change rates.
- **Contact Angle:** For condensation on solid surfaces, the contact angle between the liquid phase and the solid surface affects droplet behaviour and is considered in the simulation.
- **Surface Interaction:** Boundary conditions at the phase interface are defined to account for the interaction between the liquid and solid surfaces. This includes modelling of wetting behaviour, essential for accurate condensation simulations on surfaces.

Multiphase Surfactant Models with Adsorption/ Desorption: Addressing complex emulsion problems.

Multiphase surfactant models with adsorption/desorption play a crucial role in Computational Fluid Dynamics (CFD) simulations, particularly in scenarios involving complex fluid interfaces, such as emulsions and foams. These models are essential for understanding the behaviour of surfactants, which are molecules that can lower the surface tension between two phases. Applications are numerous:

- **Oil Industry:** Surfactant flooding in enhanced oil recovery, where surfactants modify the interfacial tension between oil and water, facilitating oil displacement.
- **Food and Beverage:** Modelling emulsification and foam stability in food processing, ensuring product quality and texture.
- **Pharmaceuticals:** Understanding surfactant behaviour in drug formulations, ensuring the stability and efficacy of pharmaceutical products.

Researchers and engineers use these models to optimize formulations, design processes, and innovate in various fields.

- **Adsorption:** Surfactant molecules adsorb onto the interface between immiscible phases, altering the surface tension and stabilizing emulsions or foams.
- **Desorption:** Surfactants can also desorb from the interface back into the bulk phases, affecting the stability of the multiphase system.
- **Phases:** CFD models consider multiple phases (e.g., oil, water, gas) and include surfactant species, treating them as additional components in the system.
- **Equilibrium Modelling:** Surfactant equilibrium between the bulk phases and the interface is crucial, and it's described using adsorption and desorption isotherms.
- **Mass Transfer:** Surfactant transport between the bulk phases and the interface is modelled, considering diffusion, convection, and the effects of interfacial curvature.
- **Adsorption Kinetics:** The rate at which surfactants adsorb to the interface is modelled, often considering kinetic adsorption/desorption models.
- **Interfacial Tension:** Surfactant models modify interfacial tension based on the concentration of surfactant molecules at the interface.
- **Marangoni Effect:** Surfactant concentration gradients at the interface can drive fluid motion (Marangoni effect), influencing flow patterns in multiphase systems.
- **Emulsion Stability:** Surfactant models help predict and optimize the stability of emulsions, preventing phase separation and coalescence of droplets.
- **Foam Stability:** Surfactant concentration gradients in foams influence bubble size distribution and foam stability, vital in industries like food and pharmaceuticals.

Improved CICSAM Model

A less diffusive version of the original CICSAM (Compressive Interface Capturing Scheme for Arbitrary Meshes) algorithm has been developed to enhance accuracy.

Height-Function Technique

Surface tension plays a vital role in simulating fluid interfaces, especially when dealing with phenomena such as capillary waves, droplet formation, and liquid-solid interactions. The height-function technique enhances the VOF method's ability to handle surface tension effects. It minimizes spurious pressure currents and enhances the computation of surface tension effects by providing a reliable way to calculate interface curvature. This accurate curvature information is vital for simulating various fluid phenomena where surface tension plays a significant role. Researchers and engineers use this technique to achieve more precise and physically meaningful simulations in multiphase flow scenarios.

Dynamic Contact Angle

When it comes to simulating dynamic contact angles using the VOF method, it involves understanding how the contact angle changes over time as a droplet or bubble moves on a solid surface. The contact angle is the angle at which a liquid/vapor interface meets a solid surface. It's a crucial parameter in understanding wetting behaviour. A static contact angle refers to the angle formed when a droplet is in equilibrium on a solid surface. Dynamic contact angle, on the other hand, refers to the angle formed when the droplet is in motion.

Dynamic Contact Angle in VOF: Achieving accurate dynamic contact angles in VOF simulations can be challenging due to the inherent numerical diffusion of the interface. Numerical diffusion causes the interface to spread over several grid cells, making it difficult to precisely capture the contact angle.

Contact Angle Boundary Conditions: Specific boundary conditions can be applied to mimic the contact angle behaviour. One commonly used condition is the "partial slip" or "no-slip" condition, where the velocity of the fluid at the solid surface is adjusted to match the desired contact angle. This helps in maintaining the contact angle during simulations.

Surface Tension Models: Including surface tension effects in a simulation can help maintain dynamic contact angles. Surface tension tends to pull the interface into a shape that minimizes the surface area, affecting the contact angle in the process. Achieving accurate dynamic contact angles in VOF simulations requires balancing numerical stability, grid resolution, and physical accuracy. It's an active area of research, and ongoing efforts are made to improve the fidelity of dynamic contact angle simulations in multiphase flow models like VOF. Researchers often validate their simulations against experimental data to ensure their models accurately represent real-world scenarios.

Level Set Method

The Level Set Method is a numerical technique used in CFD (Computational Fluid Dynamics) to simulate and analyze complex multiphase flows. It's particularly useful for tracking interfaces between different fluids in a computational domain. These developments not only cater to industry demands but also hold immense potential in academia. We recognize the strong demand for advancements in multiphase flow, and our collaborative efforts are dedicated to meeting these needs head-on.

- **Implicit Interface Representation:** The Level Set Method represents the interface between different fluids implicitly using a scalar field called the "level set function."
- **Sign Function:** The level set function assigns positive or negative values to grid points, indicating whether a point is inside or outside the fluid interface. The zero level set represents the interface itself.
- **Topology Change:** One significant advantage of the Level Set Method is its ability to handle topology changes naturally, such as merging and breaking apart of fluid phases
- **Versatility:** It is versatile and applies to various interface types, including free surfaces, bubbles, and droplets.
- **Advection:** The level set function is advected using the velocity field of the fluid. It moves with the flow, preserving the topology of the interface.
- **Re-initialization:** Over time, numerical errors might cause the level set function to lose its properties. Re-initialization methods ensure that it remains a signed distance function, enhancing accuracy and stability.
- **Interface Capturing:** The level set function is used to identify regions where the interface exists. For example, when simulating water and air, the interface corresponds to the region where the level set function is close to zero.
- **Re-distancing:** Re-distancing methods update the level set function to maintain its accuracy as a signed distance function. It ensures that the interface is accurately represented and that numerical errors are corrected.
- **Surface Tension:** The level set method can be combined with other techniques such as VOF to compute surface tension effects accurately, impacting the behaviour of droplets and bubbles.
- **Curvature Calculation:** The gradient of the level set function provides the normal vector to the interface. This information is crucial for calculating curvature and, in turn, various interfacial forces.

We look forward to this exciting journey shaping the future of CFD. The continued support and collaboration of our users and others are instrumental in driving these innovations forward.

Modelling Polymer Resin Flow and Heat Transfer in a Coat-Hanger Slot Die

by Toshiyuki Suzuki, CHAM Japan, and Michael Malin, CHAM UK

Introduction

In the polymer-processing industries, coat-hanger slot dies are used extensively for the extrusion of wide uniform sheets of polymer melts. The objective of an extrusion die is to distribute the polymer melt in the flow channel so that the material exits from the die with a uniform velocity and temperature, and minimal pressure drop. It is also important to know the flow characteristics of the polymer resin flow during extrusion molding so as to improve the product surface properties and quality by avoiding problems such as distortion and warping.

PHOENICS can assist the design process by simulating the flow through the die to investigate changes aimed at improving product quality, process performance and efficiency. Such changes include modifications to the die geometry, varying the operating parameters and using different material properties. Aside from geometrical complexity, another challenge to simulating the flow in a die is that the polymer-resin flow is non-Newtonian in nature. In particular, the flow exhibits shear-thinning behaviour, which means the apparent viscosity of the polymer decreases with shear rate.

PHOENICS is used to calculate both the flow and heat transfer through a typical coat-hanger slot die. The purpose of these preliminary simulations is to build and test a basic CFD model of the die with the ultimate objective of assisting the design process in obtaining a uniform flow and temperature distribution across the die exit, whilst minimizing the pressure drop.

Non-Newtonian Rheology Model

The rheological behaviour of thermoplastics shows a strong dependence on both temperature and shear rate, and many different models can be found in the literature. In the present work, a temperature-dependent, pseudoplastic power-law model was used to describe the rheology of the polymer flowing inside the die cavity. Figure 1 shows that the pseudoplastic fluid is characterized by a constant apparent viscosity at low shear rates, a viscosity which decreases with shear rate at intermediate rates, and a viscosity that is essentially constant again at very high shear rates. This means that the fluid has Newtonian behaviour at low and high shear rates, but exhibits shear-thinning behaviour in the transition region due to structural changes in the polymer chains.

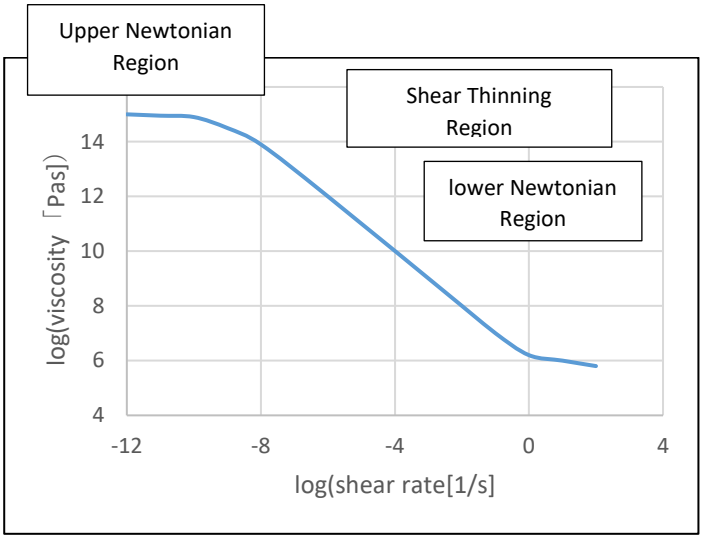

Figure 1 A typical apparent-viscosity curve for thermoplastics

In the PHOENICS model, the apparent dynamic kinematic viscosity η of the polymer melt is computed from the following equations:

When $\eta < \eta_0$

$$\eta = K\dot{\gamma}^{b-1} f_T \qquad (1)$$

When $\eta \geqq \eta_0$

$$\eta = \eta_0 \qquad (2)$$

with

$$\eta_0 = \eta_{0,T_r} f_T \qquad (3)$$

and

$$f_T = e^{-c(T-T_r)} \qquad (4)$$

In the above, K is the consistency (in Pa.s^b); γ is the shear rate (in s^{-1}); b is the flow behaviour index, which has a value less than unity for pseudoplastics; η_{0,T_r}, is the zero-shear viscosity at T_r [Pa.s], which has a limiting value of 10^{10} in PHOENICS by default; f_T is the temperature function; c is the temperature index (in 1/°C); and T_r is the reference temperature (in °C or K).

The use of the zero-shear viscosity prevents the viscosity from increasing infinitely when the shear rate is low, and so acts to increase numerical stability under these conditions. Of course, a real fluid has a maximum apparent viscosity at rest rather than the PHOENICS default of 10^{10}.

Flow Geometry and Boundary Conditions

Figure 2 shows the flow geometry of the coat-hanger die in the PHOENICS solution domain; and one-half symmetry is exploited in the depth (z) direction. The molten resin, heated to 240°C, flows into the upper part of the die, and is extruded through the slit shape in the lower half. The surrounding mould material is maintained at a temperature of 300°C, which increases the temperature of the incoming resin, which itself enters with an inflow velocity of 0.1 m/s.

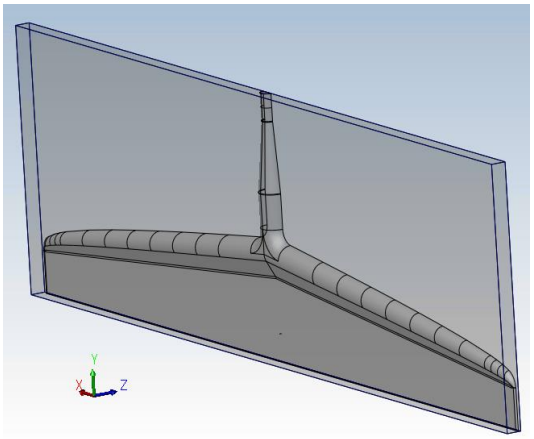

Figure 2. The coat-hanger slot die and solution domain.

Three PHOENICS simulations are performed, each with differing rheology, as defined by the following cases:

a) a uniform value of η obtained from the zero-shear viscosity at the inlet temperature.
b) a temperature-independent power-law viscosity; and
c) a temperature-dependent power-law viscosity, as given by equations (1)-(4) with T_r equal to the inlet temperature, and a temperature power index, c=0.1.

Results and Discussion

Figures 3, 4 and 5 present contours of temperature, velocity, and pressure, respectively, for each rheological model, at the central cross section of the die.

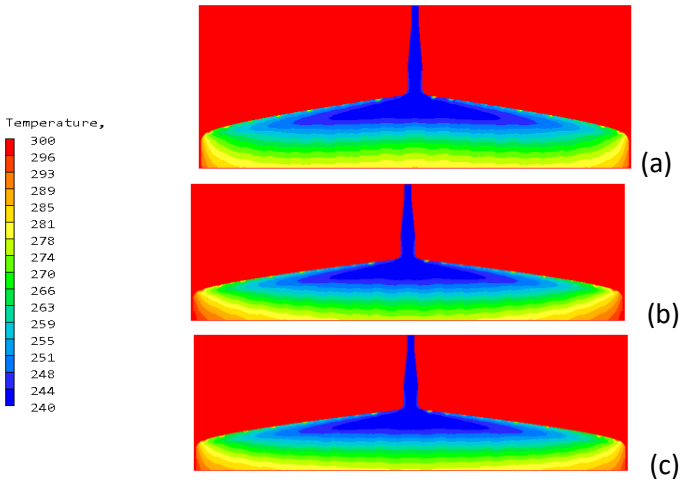

Figure 3: Temperature distributions for (a)constant η (b)Power-law, temperature-independent η (c)Power-law, temperature-dependent η.

It can be seen from Figure 3 that the temperature distribution doesn't differ much with changing rheology model. However, in contrast, the pressure distribution changes significantly, as shown in Figure 5. An important observation is that by accounting for a temperature-dependent viscosity, the predicted pressure loss decreases because the apparent viscosity decreases with increase in resin temperature.

In comparing the presence and absence of temperature dependence in the modelling, it can be seen from Figure 4 that the velocity difference between the centre and the edge of the slit is larger when there is no temperature dependence.

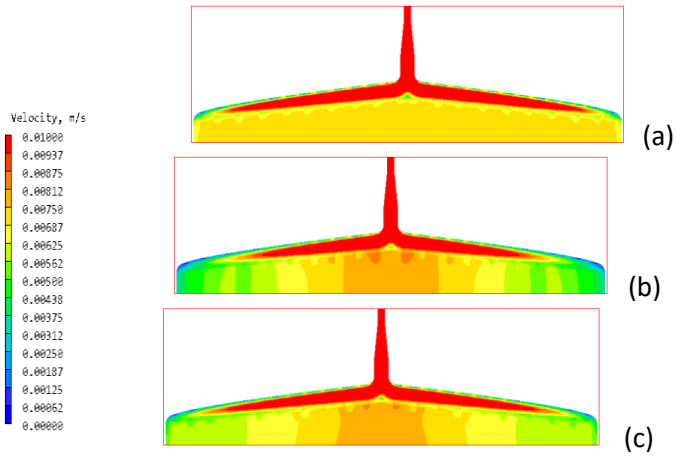

Figure 4: Velocity distributions for (a) constant η (b) Power-law, temperature-independent η (c) Power-law, temperature-dependent η.

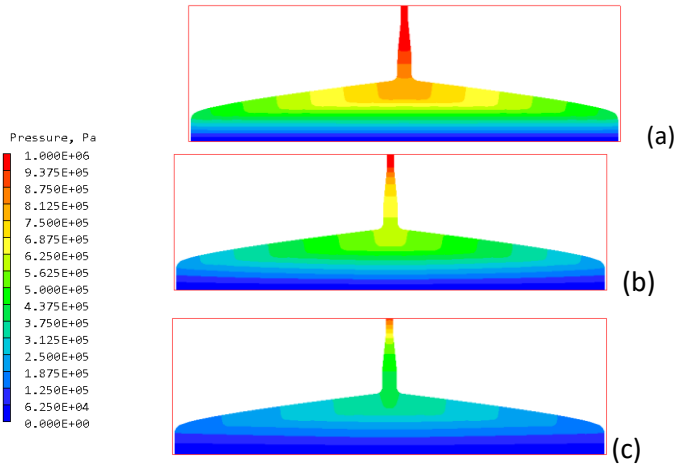

Figure 5: Pressure distributions for (a) constant η (b) Power-law, temperature-independent η (c) Power-law, temperature-dependent η.

Figures 6 and 7 show outlet distributions of temperature and pressure, respectively, predicted by each rheological model.

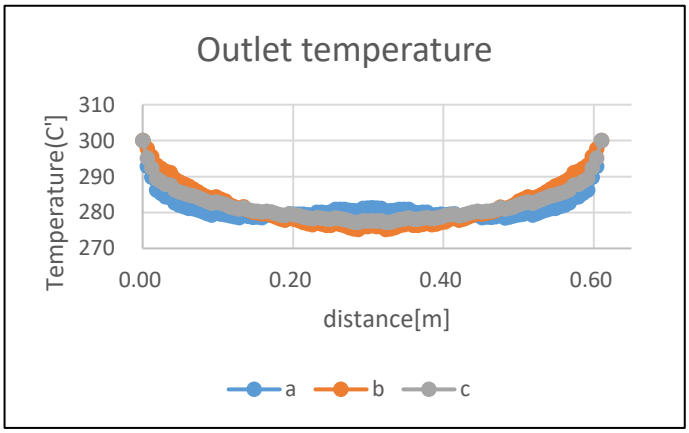

Figure 6 Difference in exit temperature due to viscosity-calculation method

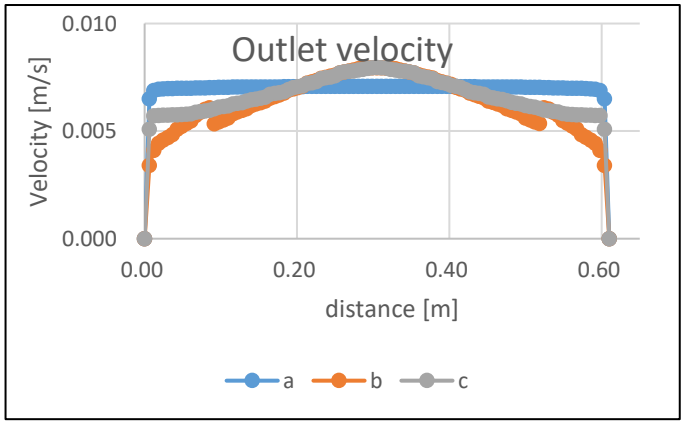

Figure 7 Difference in exit velocity due to viscosity-calculation method

Conclusions

Preliminary PHOENICS simulations have been performed of resin flow inside a coat-hanger die using a constant apparent viscosity, and a power-law model both with and without temperature dependence. The results of these simulations were compared and reported on in terms of the velocity, pressure and temperature distributions. These preliminary results were realistic as regards the predicted effects of using non-Newtonian rheology with temperature dependence.

It is now possible to perform more detailed resin flow calculations, but using more realistic and general rheological models. This will be done in future work by using models such as the Carreau and Cross models, which smoothly describe the transition between the upper and lower Newtonian regions of shear-thinning fluids. Both of these models, among others, are now readily available in PHOENICS as switch-on options [1]. Other future avenues of work will include extending the PHOENICS CFD model to allow for concentration dependence, which is needed to simulate cases where resins of different materials are laminated to form a resin film.

References

1. Non-Newtonian Fluids, https://www.cham.co.uk/phoenics/d_polis/d_enc/non.htm

Some New Items in PHOENICS 2023: For a full list, and a list of bug fixes, please contact CHAM

- Steady state VOF
- Pasquil stability criteria in WIND object
- Ergun and porous material pressure drop via GUI for domain-material BLOCKAGE
- Logarithmic contour plots in VRV
- Much of the VTK display is already incorporated into the development code, but it is not complete.
- Ability to overwrite solution file(phida/phi) when saving intermediate fields in steady state
- Improvements to convergence monitor:
  - ability to 'pin' display of figures for each plot
  - ability to highlight individual curves by selecting them
  - ability to save and load convergence monitor layout
  - elapsed time and estimated times show minutes & seconds for short runs
- USP extension
  - Physical property formulae used in PROPS file.
  - FLAIR Comfort Indices.
  - Heat source on outside of 198 blockages.
  - Compressible / high speed flow
    - Wind object.
    - Fire object.
    - Full reporting of sources in result as in SP
    - Realisable k-ε τurbulence model

CO_2 Distribution under CO_2 Enrichment using CFD considering Photosynthesis in a Tomato Greenhouse

by Moliya Nurmalisa, Takayuki Tokairin, Tadashi Kumasaki, Kotaro Takayama* and Takanobu Inoue

Toyohashi University of Technology, Toyohashi 4418580, Japan; * Ehime University, Matsuyama 7908577, Japan

1) Introduction

Carbon dioxide (CO_2) enrichment (also called supplementation) is the process of adding more CO_2 into a greenhouse to improve plant growth and production by increasing photosynthesis in plants. CO_2 is essential to photosynthesis, which is a chemical process that uses light energy to convert CO_2 and water into food for plants. Most greenhouse plants require a minimum concentration of about 330 mg/l to enable them to photosynthesize efficiently enough to grow and develop normally. For this reason, a greenhouse should be designed to replenish CO_2 levels to at least this level during day time, but it is well known that increasing CO_2 levels further through supplementation will increase plant growth rates and yields.

It is challenging to maintain an optimal CO_2 concentration in a greenhouse because of the impact of temperature, humidity, light intensity and air circulation. Computational Fluid Dynamics (CFD) is a tool that can be used to investigate suitable climate-regulation designs by simulating the conditions inside greenhouses and other cultivation facilities. Since the 1990s, CFD has been used extensively for these applications [1], although largely, photosynthesis modelling has been considered only in more recent CFD studies [1-3]. Consequently, there have been very few CFD studies where photosynthesis was included when predicting CO_2 distribution and enrichment in a greenhouse.

The objective of the present study is to predict the detailed CO_2 distribution within a greenhouse by using a PHOENICS-based CFD model, which considers CO_2 enrichment and photosynthesis modelling with CO_2 absorption. The study is conducted in two stages. First, the CFD model is verified by comparing CFD simulations with the CO_2 levels measured in a semi-closed, hanging, photosynthetic chamber [3] located in a greenhouse.

The CFD model is then used to calculate and verify the precise CO_2 distribution inside a greenhouse, where CO_2 enrichment is supplied from a system of perforated tubes. A few greenhouse simulations are then conducted to determine the impact of various environmental factors on the CO_2 distribution, including the use of side vents, which can be opened or closed; and differing weather conditions, which can be either sunny or rainy. This article focusses on the greenhouse simulations, and so the reader is directed elsewhere [4] for details on successful simulations of the photosynthetic chamber.

2) The CFD Model

Greenhouse Geometry and Solution Domain

Figure 1 shows the vinyl greenhouse located at Toyohashi University of Technology, Japan. The greenhouse has a plan area of 120 m^2, corresponding to the following dimensions: length 12m, width 10m, height 6.03m. The greenhouse has four circulating fans, four shelves of cultivating bed for tomato, and four perforated CO_2 tubes on each shelf. The CFD solution domain is shown in Figure 2. Leakage paths were managed in the door area and in tiny gaps across the greenhouse rib structure between the wall and the roof.

Figure 1. The greenhouse for CO_2 measurement.

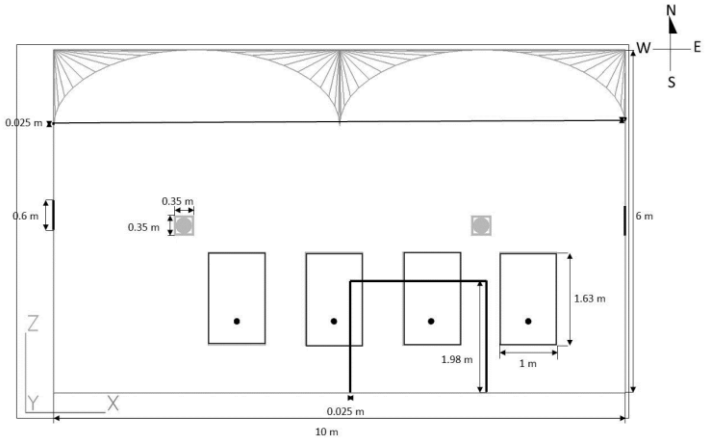

Figure 2. Greenhouse CFD model: - the squares represent fan circulator, rectangular shapes represent the plants, the circles represent perforated CO_2 tubes, and the thick lines and dots represent the outlet.

3) Computational Details

The greenhouse simulation was conducted using the standard k-ε turbulence model and the predictions were compared with the measured data of CO_2 enrichment [5]. Table 1 presents the computational details for the three-dimensional CFD simulation.

A mesh of 739,350 cells was used inside the greenhouse, as indicated in Figure 3. The accuracy of the CFD model was assessed by using root mean-square error (RMSE) and mean-absolute percentage error (MAPE) comparisons at each measured and simulated point.

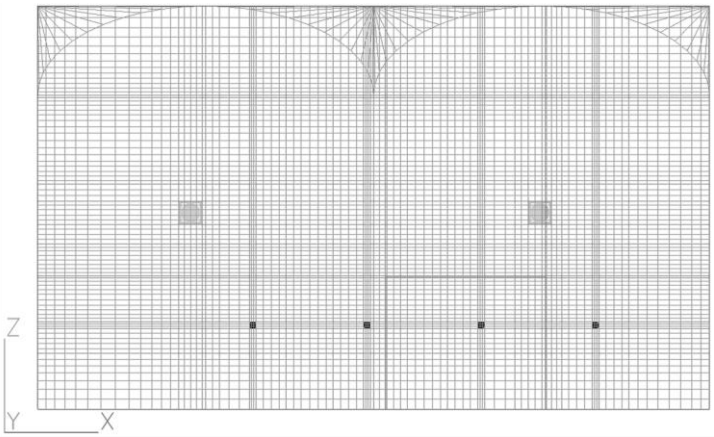

Figure 3. Meshing for the greenhouse model: - the four rectangular shapes inside the chamber represent the plants, the circles represent perforated CO_2 tubes, and the squares represent fans.

Further details of the PHOENICS-based CFD model, such as for example, the modelled equations and photosynthesis model, are reported in the original publication [4].

Table 1. Computational details used for the greenhouse model

Parameter	Symbol	Unit	Value
Canopy photosynthesis rate	P_{cg}	$g\ CO_2\ h^{-1}\ m^{-2}_{ground\ area}$	
CO_2 density	Cc	$g\ m^{-3}$	1839
Conductance of CO_2	τ_c	$m\ s^{-1}$	12.168×10^{-4}
Crop respiration	R`	$g\ h^{-1}\ m^{-2}$	2.84×10^{-2}
Initial CO_2	-	ppm	450
Leaf area density	LAD/??	$m^2_{leaf}\ m^{-3}_{row}$	0.67
Leaf area index	LAI	$m^2\ m^{-2}$	1.1
The light use efficiency of the plant canopy	α_c	$g\ CO_2\ J^{-1}$	3.705×10^{-6}
The incident light flux PAR	J_o	$W\ m^{-2}_{leaf}$	355

4) Results and Discussion

In this section, only a sample of the experimental and predicted results are considered, and the reader is referred to Nurmalisa et al [3] for a full description, including the detailed comparisons made between measured and predicted CO_2 values.

CO_2 distribution inside the greenhouse: In the present study, the simulation results were compared with the measurement data [5] of CO_2 concentration for conditions 20 min after an hour's supply of CO_2 at the middle canopy, 1.2 m above the ground, as shown in Figure 4. The initial field values of CO_2 concentration were assumed uniform throughout the greenhouse, whereas under actual conditions, there are varying CO_2 concentrations.

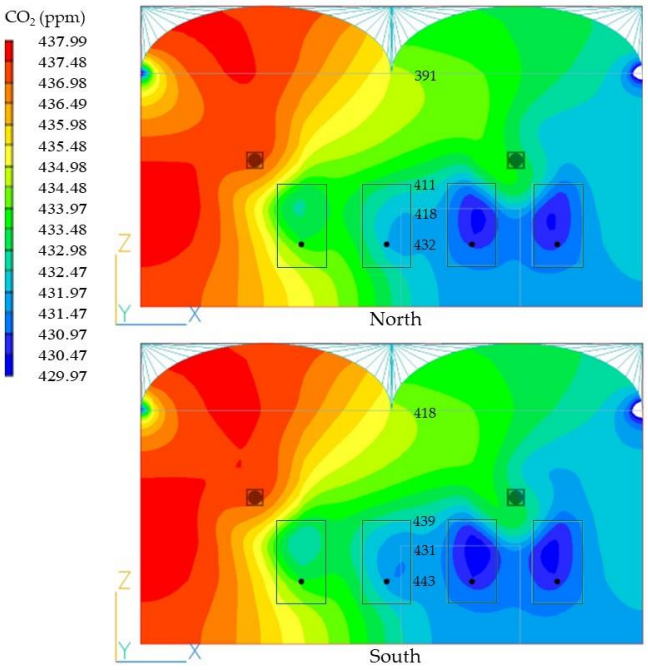

Figure 4. CO_2 distribution inside the greenhouse considering CO_2 absorption through photosynthesis by plants (image taken at cross-section 3.4 m from south wall).

Simulation cases for greenhouse model

Several simulations were conducted to analyze CO_2 distribution under the CO_2 enrichment, as described below.

CO_2 distribution toward open and closed side ventilation inside the greenhouse: Figure 5 shows the predicted CO_2 distributions for the cases of open and closed side vents. The results show a slight difference in CO_2 concentration, with the closed-vent case showing slightly higher values. Figure 5 (side ventilation open) showed that the CO_2 concentration around the plants (rectangular shapes) was still maintained higher than the ambient CO_2 concentration of about 400 ppm. This suggests that practical CO_2 enrichment was still effective, even if the side vent was open.

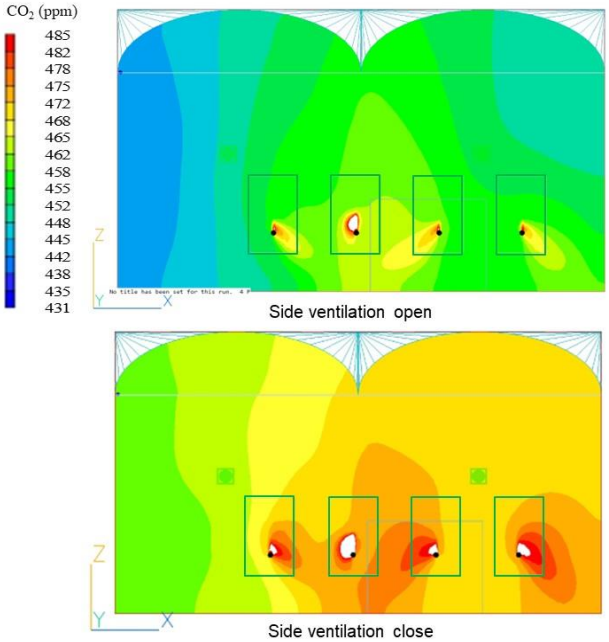

Figure 5. CO_2 distribution inside the greenhouse for the case of side ventilations open and closed (image taken at cross-section 6 m from south wall)

CO_2 distributions inside the greenhouse on a sunny and rainy day: Simulations under treatment of 1000 ppm of CO_2 concentration were conducted for rainy- and sunny-day conditions with PAR (Photosynthetically Active Radiation) values [3,6] of 95 W m^{-2} [3,6], and 355 W m^{-2}, respectively. These PAR values are based on the NEDO (New Energy and Industrial Technology Development Organization) solar-radiation database. The results shown in Figure 6 reveal that there was a minor change in CO_2 concentration between sunny and rainy days.

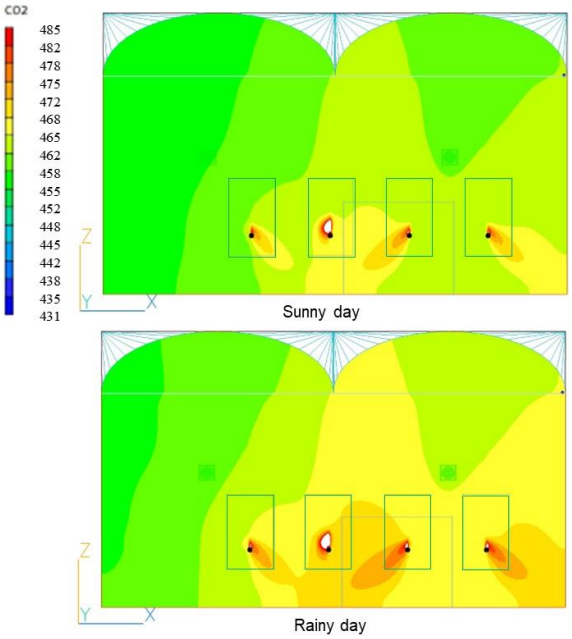

Figure 6. CO_2 distribution inside of the greenhouse for the case of sunny and rainy day (image taken at a cross-section 6 m from south wall).

Discussion: This study presented numerically the details of CO_2 distribution inside the greenhouse. The model reproduced the distribution of measured CO_2 concentration in the middle of the plant, decreasing due to CO_2 absorption by photosynthesis. The greenhouse-simulation results at the bottom of canopy showed good agreement with the measurements. At the location of 3.4 m from north wall, the predictions overestimated the measured results; whereas 3.4 m from south wall, the data were slightly underestimated for heights of 1.2 m and 2.4 m above the ground. For heights of 1.8 m and 4.2m, the data were over predicted by the model. This may be because temperature variations were neglected in the simulations. However, the CFD model was still able to predict the detailed CO_2 distribution, with account taken of CO_2 absorption at the plant by photosynthesis. Furthermore, the error values were still reasonable compared to those reported in previous studies.

A few simulations were conducted to determine the effect of various environmental conditions on the CO_2 distribution inside the greenhouse. Cases with open and closed side vents showed that closed side vents have a slightly more even CO_2 concentration than those with open side vents inside the greenhouse. By contrast the variability of CO_2 inside the plant, open (8.8%) and closed (8.7%) side vents, induced almost no significant improvement. Additionally, cases of a rainy- and sunny-day model showed that photosynthetically active radiation possibly compensated CO_2 absorption through photosynthesis to be lower at low light (rainy day) and higher at high light (sunny day). Nonetheless, it was found that there was almost no significant difference in the variation of CO_2 concentration in the plant between rainy and sunny days.

5) Conclusions

The distributions of CO_2 in the photosynthetic chamber and greenhouse were studied using PHOENICS to understand the details of CO_2 concentration, while considering net photosynthesis. Consequently, the measured and simulated values of CO_2 concentration were well validated in this study. It was determined that there would be no discernible difference in the CO_2 distribution between models using open and closed side vents in the greenhouse, provided there was no interference with air exchange for these vents. It was found that light and CO_2 distribution have an impact on the processes involved in photosynthesis. Thus, this research could take a role supporting agricultural technology.

6) References

1. Fatnassi, H., Bournet, P.E., Boulard, T., Roy, J.C, Molina-Aiz , F.D., Zaaboul, R., *Use of computational fluid dynamic tools to model the coupling of plant canopy activity and climate in greenhouses and closed plant growth systems: A review.* Biosystems Engineering, **2023**, 388-408.
2. Molina-Aiz, F.D., Norton, T., López, A., Reyes-Rosas, A. Moreno, M.A., Marín, P., Espinoza, K., Valera, D.L. *Using computational fluid dynamics to analyse the CO_2 transfer in naturally ventilated greenhouses*. Acta Hortic. **2017**, 1182, 283–292.
3. Nurmalisa, M.; Tokairin, T.; Takayama, K.; Inoue, T. *Numerical simulation of detailed airflow distribution in newly developed photosynthesis chamber*. In Proceedings 2nd International Conference on Environment, Sustainability Issues, and Community Development (Virtual Conference), Semarang, Indonesia, 21 October **2020**.
4. Nurmalisa, M.; Tokairin, T.; Kumazaki, T.; Takayama, K.; Inoue, T. *CO_2 distribution under CO_2 enrichment using computational fluid dynamics considering photosynthesis in a tomato greenhouse*. Appl. Sci. **2022**, 12, 7756. (https://doi.org/10.3390/app12157756)
5. Kumazaki, T.; Ikeuchi, Y.; Tokairin, T. *Relationship between positions of CO_2 supply in a canopy of tomato grown by high-wire system and distribution of CO_2 concentration in a greenhouse*. Clim. Biosph. **2021**, 21, 54–59
6. Romdhonah, Y.; Fujiuchi, N.; Shimomoto, K.; Takahashi, N.; Nishina, H.; Takayama, K. *Averaging techniques in processing the high time-resolution photosynthesis data of cherry tomato plants for model development*. Environ. Control Biol. **2021**, 59, 107–115.

Internal Waves Generated by a Flexing Body

Dr. R. P. Hornby email:bob.hornby007@gmail.com

Introduction

The near surface layers of the ocean are mixed by wind driven turbulence and so are of uniform density but at deeper depths the ocean remains density stratified. The depth of the surface mixed layer in general depends on the wind strength and duration but can vary from one to hundreds of metres. Bodies that vibrate or flex (e.g. fish, submersibles) in the density stratified depths of the ocean generate internal waves which propagate away from the body and have some unusual properties. In particular internal waves from vibrating bodies propagate energy along, rather than perpendicular, to lines of constant wave phase. These properties are discussed in detail in Ref 1. In this article, PHOENICS is used to illustrate some of these properties but also to extend the analysis by using the ideas inherent in the MOFOR methodology for moving bodies (see Ref 2).

Analysis

PHOENICS is used to solve the 2-D and 3-D time dependent laminar equations of mass momentum and energy when a moving body flexes in a uniformly stratified environment. A Cartesian grid is used with the Koren differencing scheme. The local buoyancy frequency is given by

$$N = sqrt(-g\frac{\frac{d\rho}{dz}}{\rho})$$

where *g* is the acceleration due to gravity, ρ the density and *z* the vertical coordinate.

The first 2-D case considered (case 1) is for a stationery body with a vertical sinusoidal oscillation for the whole body (velocity *wb*) with frequency ω set less than *N*

$$wb = \text{asin}\,(\omega t)$$

where *a* is the amplitude and *t* the time. More complicated situations can be analysed by applying the local velocity of the cell within the body at the given frequency. For example cases can be considered with cell sinusoidal velocities within the body given by (case 2)

$$wb = \text{asin}(\omega t)\,\sin\,(\frac{2\pi xb}{L})$$

Where *xb* is the lateral coordinate in the body and *L* the body length.

Body velocities of a see/saw nature can also be analysed, for example (case 3)

$$wb = \text{asin}(\omega t)\,(1 - \frac{2xb}{L})$$

A further interesting case can be explored by considering a brief, sudden change in the velocity of the whole body (case 4)

$$wb = aexp(-\frac{\omega t}{2\pi})$$

This type of analysis can be extended to 3-D transient cases where the body has both a translation and flexing action. Then the oscillatory waves due to flexing are expected to be superimposed on the rather different waves resulting from translational motion.

Results

It can be shown (Ref 1) that waves of frequency ω less than *N* will be found in directions θ, where

$$\cos(\theta) = \frac{\omega}{N}$$

For case 1 ω is set at *N/sqrt(2)* so the expectation is for the internal wave energy to propagate at 45 degrees to the vertical. The PHOENICS results are shown in Figure 1 and compared with Schlieren experimental results (measuring density gradients) for the same frequency. There is very good agreement on the directions of wave energy propagation.

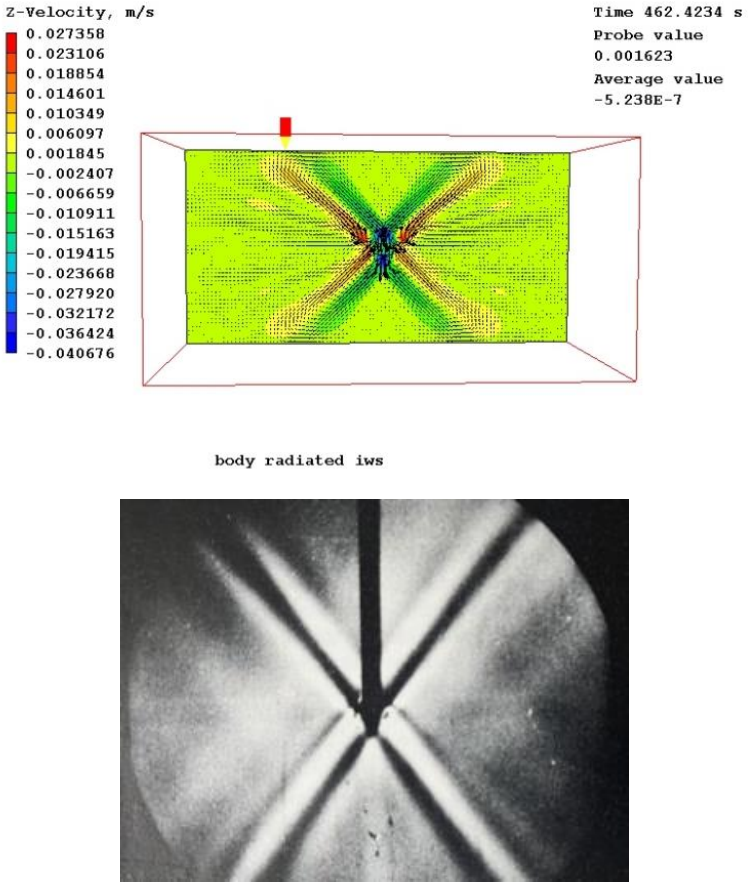

Figure 1 The top plot shows the PHOENICS velocity vectors and vertical velocity contours for a central body vibrating vertically with frequency N/sqrt(2) in a uniformly stratified fluid. On the bottom is the equivalent experimental result (taken from Ref 1 p314, figure 76, photograph by D. H. Mowbray).

Cases 2 and 3 Involve opposite motions within the body at the given frequency and so produce a more complex picture due to the phase changes across the body and the horizontal displacement of the motions. This is illustrated in Figure 2 using the case 2 velocities. Similar results are obtained using the case 3 velocities.

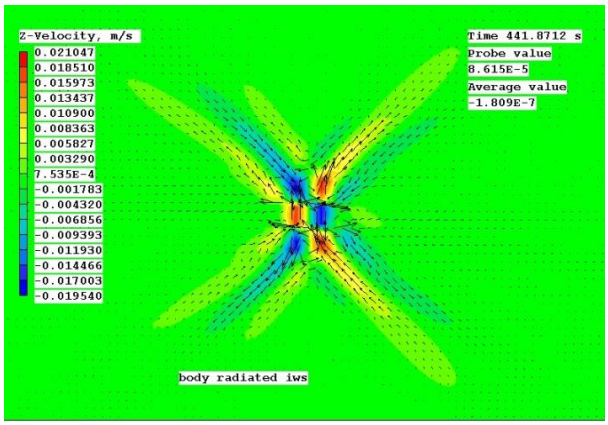

Figure 2. PHOENICS velocity vectors and contours of vertical velocity for a central body vibrating vertically with frequency N/sqrt(2) in a uniformly stratified fluid. Contours of the vertical velocity are shown to illustrate the displacement and phase effect (case 2).

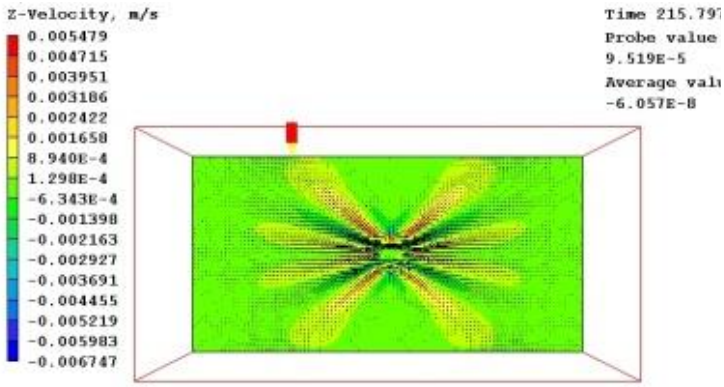

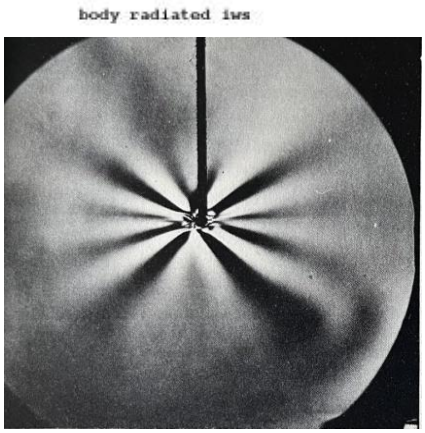

Figure 3. Top plot shows PHOENICS early time results for a brief displacement of the body (case 4). The bottom picture shows early time experimental results for a similar setup (taken from Ref 1 p315, figure 77a, photograph by T.N. Stevenson)..

Case 4 involves a sudden, brief change in the displacement of the whole body which generates various wavelengths and frequencies. Figures 3 and 4 show PHOENICS and experimental results (for a similar setup) for the wave pattern at two times from the initiation of the disturbance.

Figure 3 shows the results at an early time from the initiation of the disturbance and Figure 4 at a later time. These figures show the multiple wave rays developing due to the differing frequency content of the disturbance and the angle subtended at the source deceasing with time with the larger wavelengths travelling further in a given time. In each case the PHOENICS results are very representative of those of the experiments

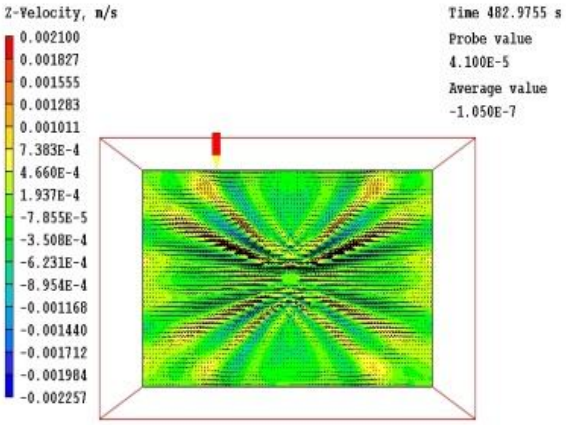

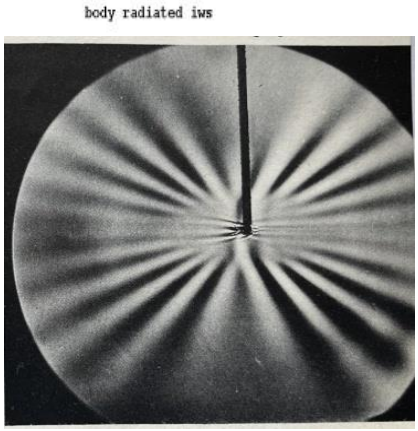

Figure 4. The top plot shows PHOENICS later time results for a brief displacement of the body (case 4). The bottom picture shows later time experimental results for a similar setup (taken from Ref 1 p315, figure 77b, photograph by T.N. Stevenson).

Conclusions

PHOENICS results have been shown for 2-D vertical oscillations of a body in a stratified fluid. The results for oscillations of a rigid body have been shown to agree well with equivalent experiments. In addition, use of the MOFOR technique allowed an extension to exploration of the body flexing; and some 2-D results of application of this technique have been shown. The method can be further extended into 3-D to investigate bodies that both translate and flex, and this will be outlined in a future article.

Referencess

1. Lighthill M J. Waves in Fluids, Cambridge University Press 1978
2. Hornby R P. PHOENICS Modelling of a Moving Body in a Stratified Tank. PHOENICS Newsletter Winter 2019.

Reactions from some Agents re the takeover by ZWSOFT:

1) **ACFDA:**
   Dear Colleen, Thank you for letting me know that CHAM has been acquired by ZWSOFT. I hope that this new structure will be successful. It has been a great pleasure for me to collaborate with you while representing CHAM in Canada and USA. It was a challenging and exciting time. Thank you very much for all your support over the past 25 years! I wish you and your family all the best! Kind regards, Vladimir
2) **ArcoFluid:**
   See Page 2
3) **Coolplug:**
   Dear Colleen, Thank you for this news. …….. this comes as a surprise to me. Good to hear that the agents' position remains unchanged. I will therefore continue my work as usual. [I was} asked to attend the BIM World event in Munich on 28-29 November. I will be happy to participate in this and I think it would be nice to get to know the people behind ZWSOFT. ……. I assume nothing will change for customers for the time being? Licence type, prices? Colleen, I wish you and your family all the best for the future. Best regards, Frank Kanters

News from CHAM:

This is the last Newsletter I will edit. Having started the original Newsletter in the e time, the PHOENICS User Club (Academic users), it became more general with various editors until, recently, it returned to me.

From the Winter Issue it will be edited by William Spalding.
Please keep contributing. All future material to newsletter@cham.co.uk.

Thank you to all who have sent material for use up to, and including, this edition. I have much enjoyed interacting with you, reading your articles, fitting them into the Newsletter and seeing them on the website.

Thank you also to all who edited, commented, corrected, and read the issues.

I look forward to reading future copies online and seeing what is happening as our Staff, our Agents, CHAM, and PHOENICS, move forward.

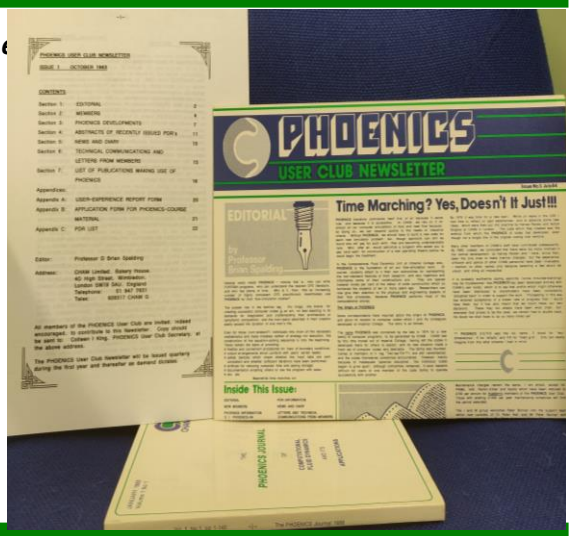

Contact Us:

CHAM's highly skilled, and helpful, technical team can assist in solving your CFD problems via proven, cost-effective, and reliable, CFD software solutions, training, technical support and consulting services. If YOU have a CFD problem why not get in touch to see how WE can help with the solution?

Please call on +44 (20) 89477651, email sales@cham.co.uk or check o(PHOENICS-OTC) call us or contact phoenics.cloud@cham.co.uk
See us on social media sites shown below:

Concentration Heat and Momentum Limited (CHAM)
Bakery House, 40 High Street
Wimbledon Village
London SW19 5AU, England